

THE LYMAN-CONTINUUM PHOTON PRODUCTION EFFICIENCY ξ_{ION} OF $Z \sim 4$ -5 GALAXIES FROM IRAC-BASED $H\alpha$ MEASUREMENTS: IMPLICATIONS FOR THE ESCAPE FRACTION AND COSMIC REIONIZATION

R.J. BOUWENS¹, R. SMIT^{1,2}, I. LABBÉ¹, M. FRANX¹, J. CARUANA³, P. OESCH³, M. STEFANON¹, N. RASAPPU¹

Draft version August 4, 2021

ABSTRACT

Galaxies represent one of the preferred candidate sources to drive the reionization of the universe. Even as gains are made in mapping the galaxy UV luminosity density to $z > 6$, significant uncertainties remain regarding the conversion to the implied ionizing emissivity. The relevant unknowns are the Lyman-continuum (LyC) photon production efficiency ξ_{ion} and the escape fraction f_{esc} . As we show here, the first of these unknowns is directly measurable in $z = 4$ -5 galaxies based on the impact the $H\alpha$ line has on the observed IRAC fluxes. By computing a LyC photon production rate from the implied $H\alpha$ luminosities for a broad selection of $z = 4$ -5 galaxies and comparing this against the dust-corrected UV -continuum luminosities, we provide the first-ever direct estimates of the LyC photon production efficiency ξ_{ion} for the $z \geq 4$ galaxy population. We find $\log_{10} \xi_{ion}/[\text{Hz ergs}^{-1}]$ to have a mean value of $25.27_{-0.03}^{+0.03}$ and $25.34_{-0.02}^{+0.02}$ for sub- L^* $z = 4$ -5 galaxies adopting Calzetti and SMC dust laws, respectively. Reassuringly, both derived values are consistent with standardly assumed ξ_{ion} 's in reionization models, with a slight preference for higher ξ_{ion} 's (by ~ 0.1 dex) adopting the SMC dust law. High values of ξ_{ion} (~ 25.5 - 25.8 dex) are derived for the bluest galaxies ($\beta < -2.3$) in our samples, independent of dust law and consistent with results for a $z = 7.045$ galaxy. Such elevated values of ξ_{ion} would have important consequences, indicating that f_{esc} cannot be in excess of 13% for standard assumptions about the faint-end cut-off to the LF and the clumping factor.

Subject headings: galaxies: evolution — galaxies: high-redshift

1. INTRODUCTION

One of the biggest longstanding puzzles regards the reionization of the universe. While we have general knowledge of the broad time scale over which reionization has occurred, many important issues remain unclear. For example, there continues to be a debate about which sources drive reionization (e.g., Robertson et al. 2015; Madau & Haardt 2015). Similarly, we have limited information about the precise epoch when reionization is completed and also how rapidly the universe transitions from a largely neutral state to the $\sim 30\%$ ionized filling factors being inferred at $z \sim 8$ (Schenker et al. 2014; Robertson et al. 2015; Bouwens et al. 2015b; Mitra et al. 2015; Ishigaki et al. 2015; Finkelstein 2015).

In the last year, new estimates of the Thomson optical depths ($\tau = 0.066 \pm 0.016$) have become available thanks to an analysis of the results from the Planck mission (Planck Collaboration 2015) and are consistent with the cosmic ionizing emissivity being somewhat lower than what had previously been inferred from analyses of the WMAP τ measurements (e.g., Kuhlen & Faucher-Giguère 2012; Haardt & Madau 2012; Bouwens et al. 2012a; Alvarez et al. 2012; Robertson et al. 2013). These new results point towards the cosmic ionizing emissivity evolving very similarly to the UV -continuum luminosity

density (Robertson et al. 2015; Bouwens et al. 2015b; Mitra et al. 2015; Choudhury et al. 2015).

In calculating the ionizing emissivity derived from galaxies, three factors are standardly included in the calculation (e.g., Kuhlen & Faucher-Giguère 2012; Robertson et al. 2013): the galaxy UV luminosity density ρ_{UV} , the escape fraction f_{esc} , and the Lyman-continuum photon production efficiency ξ_{ion} (describing the production rate of Lyman-continuum ionizing photons per unit luminosity in the UV -continuum). While most of the effort has been devoted to improving current constraints on the UV luminosity density ρ_{UV} and the escape fraction f_{esc} , the Lyman-continuum photon production efficiency ξ_{ion} is also fairly uncertain. In general, estimates of this efficiency ξ_{ion} appear to be exclusively indirect, based on the UV -continuum slope β of galaxies using standard stellar population models (Robertson et al. 2013; Duncan & Conselice 2015; Bouwens et al. 2015b, 2015c) or using predictions for young stellar populations that are possibly subsolar (e.g., Madau et al. 1999; Schaerer 2003).

Despite these indirect attempts to constrain ξ_{ion} , many recent observations are now providing constraints on the $H\alpha$ fluxes of $z \sim 4$ and $z \sim 5$ galaxies based on the impact of $H\alpha$ and other nebular lines to the IRAC fluxes (Schaerer & de Barros et al. 2009; Shim et al. 2011; Stark et al. 2013; de Barros et al. 2014; Laporte et al. 2014; Rasappu et al. 2015; Smit et al. 2015a,b; Marmol-Queralto et al. 2015). As the observed $H\alpha$ fluxes can be directly related to the total number of Lyman-continuum photons produced by stars in a galaxy (assuming an escape fraction of zero: e.g., Leitherer & Heckman 1995), we can use the observed $H\alpha$ and UV -continuum fluxes of distant galaxies to set constraints on ξ_{ion} . In a related

¹ Leiden Observatory, Leiden University, NL-2300 RA Leiden, Netherlands

² Centre for Extragalactic Astronomy, Durham University, South Road, Durham, DH1 3LE, UK

³ Institute of Space Sciences & Astronomy, University of Malta, Msida MSD 2080, Malta

⁴ Yale Center for Astronomy and Astrophysics, Yale University, New Haven, CT 06520, USA

investigation, Stark et al. (2015) recently showed how one could use measurements of the flux in the CIV λ 1548 line for a lensed Lyman-break galaxy at $z = 7.045$ to constrain $\log_{10} \xi_{ion}/[\text{Hz ergs}^{-1}]$, estimating it to be $25.68^{+0.27}_{-0.19}$.

Here we derive constraints on the Lyman-continuum photon production efficiency ξ_{ion} by making use of a large sample of star-forming galaxies distributed over the redshift range $z = 3.8\text{-}5.4$, where we know the passband in which the H α emission likely falls. We obtain these samples thanks to the recent work of Smit et al. (2015b) and Rasappu et al. (2015), where spectroscopic redshift $z = 3.8\text{-}5.4$ samples are supplemented with photometric redshift samples. In each case, the H α emission line lies in one of the two IRAC filters, with no prominent contribution from other nebular lines. As we will see (§3) and as demonstrated by the results presented in Smit et al. (2015b), these spectroscopic and photometric samples exhibit similar H α EWs but have complementary strengths (i.e., spectroscopic-redshift samples provide a sampling of galaxies with more secure redshifts while photometric redshift samples likely provide a more representative sampling of UV-bright galaxies, with less bias towards line emitters).

The plan for this paper is as follows. We begin (§2) by briefly summarizing the observational data sets and selection criteria. In §3, we describe the methodology we utilize in Smit et al. (2015b) for deriving the H α fluxes for individual sources in our different samples. We then use these H α fluxes to estimate the Lyman-continuum photon production efficiency ξ_{ion} for individual sources and then look at how ξ_{ion} depends on the UV luminosity, the UV-continuum slope, and redshift. We then combine these measurements with results available on the total ionizing emissivity at $z \sim 4\text{-}5$ to set an upper limit on the escape fraction of galaxies to 13%. In §4, we discuss the implications of the present results and then conclude (§5). Where necessary, we assume $\Omega_0 = 0.3$, $\Omega_\Lambda = 0.7$, and $H_0 = 70 \text{ km/s/Mpc}$. All magnitudes are in the AB system (Oke & Gunn 1983).

2. OBSERVATIONAL DATA AND SAMPLE SELECTION

In the present section, we provide a brief summary of both the observational data sets and selection criteria we utilize for deriving our results. As we use the $z = 3.8\text{-}5.4$ samples and IRAC photometry from Smit et al. (2015b) and Rasappu et al. (2015), we refer the interested reader to those papers for more details.

2.1. Observation Data

For our source selection and photometry, we utilize the deep HST optical and near-infrared observations over the two GOODS fields. Over those fields, we make use of almost all optical/ACS and near-infrared/WFC3/IR observations, including observations from the original ACS GOODS and follow-up program (Giavalisco et al. 2004), the ERS program (Windhorst et al. 2011), and the CANDELS program (Grogin et al. 2011; Koekemoer et al. 2011). Collectively, the data from these programs generally reach to $>\sim 27 \text{ mag}$ at 5σ all the way from optical wavelengths at $0.4\mu\text{m}$ to the near-infrared $1.6\mu\text{m}$. Moderately deep observations ($\sim 25.0\text{-}25.5 \text{ mag}$; 5σ) in the K -band are available over $>90\%$ of the two CANDELS fields.

For the Spitzer/IRAC observations needed for our H α flux estimates, we utilize the new reductions from Labbé et al. (2015), who have incorporated the full set of observations from the original GOODS, SEDS (Ashby et al. 2013), S-CANDELS (Ashby et al. 2015), and IUDF programs (Labbé et al. 2015). These reductions feature a PSF with a $1.8''$ FWHM, $\sim 10\%$ sharper than achieved in most analyses, due to the use of a drizzle methodology for coadding the Spitzer/IRAC observations.

2.2. Selection of Spectroscopic Sample

A large number of spectroscopic redshifts have been derived over the GOODS-North and South over the last ten years and made public in many independent efforts (Vanzella et al. 2005, 2006, 2008, 2009; Balestra et al. 2010; Shim et al. 2011; Stark et al. 2010, 2011, 2013; Rasappu et al. 2015).

In Smit et al. (2015b) and Rasappu et al. (2015), we took advantage of several public spectroscopic redshift compilations (Vanzella et al. 2009; Shim et al. 2011; Stark et al. 2013) to construct a sample of $z = 3.8\text{-}5.0$ galaxies and $z = 5.1\text{-}5.4$ galaxies, while also benefitting from some $z = 5.1\text{-}5.4$ sources from Stark et al. (2015, in prep). For the first redshift subsample, the H α line falls squarely in the Spitzer/IRAC $3.6\mu\text{m}$ filter, and in the second subsample, the H α line falls in the Spitzer/IRAC $4.5\mu\text{m}$ filter.

2.3. Selection of Photometric Sample

Following the treatment in Smit et al. (2015b) and Rasappu et al. (2015), we also consider a selection of sources which very likely lie in the redshift intervals $z = 3.8\text{-}5.0$ and $z = 5.1\text{-}5.4$, respectively (99% and 85%), according to their photometric constraints. Rasappu et al. (2015) only required sources to show an 85% likelihood of lying in the target redshift interval ($z = 5.1\text{-}5.4$) to compensate for the greater difficulty of isolating a source photometrically to such a narrow interval in redshift.

Selecting sources according to their redshift likelihood distribution is useful, since it allows us to be more inclusive in our selection of $z \sim 4\text{-}5$ galaxies and not to base the results on sources which only show Ly α in emission. This is to address the concern that such samples may be biased towards sources with younger ages and not be totally representative.

3. EMPIRICAL ESTIMATE OF ξ_{ION}

3.1. Measurement of H α Fluxes

The H α flux measurements we utilize in this study are directly taken from Smit et al. (2015b) and from Rasappu et al. (2015), so we refer our audience to their studies for a detailed description. Nevertheless, our basic methodology is as follows. To begin, we derive a detailed SED fit to the full photometry we have available (HST + ground-based K_s + Spitzer/IRAC) for all sources in our samples to obtain good constraints on the overall shape of the spectral energy distribution, excluding the Spitzer/IRAC passband we expect with high confidence to contain the H α emission line. We then compare the measured flux of sources in the Spitzer/IRAC $3.6\mu\text{m}$ or $4.5\mu\text{m}$ band with the model flux expected in that band based on our best-fit SED (and not including line flux in the SED model).

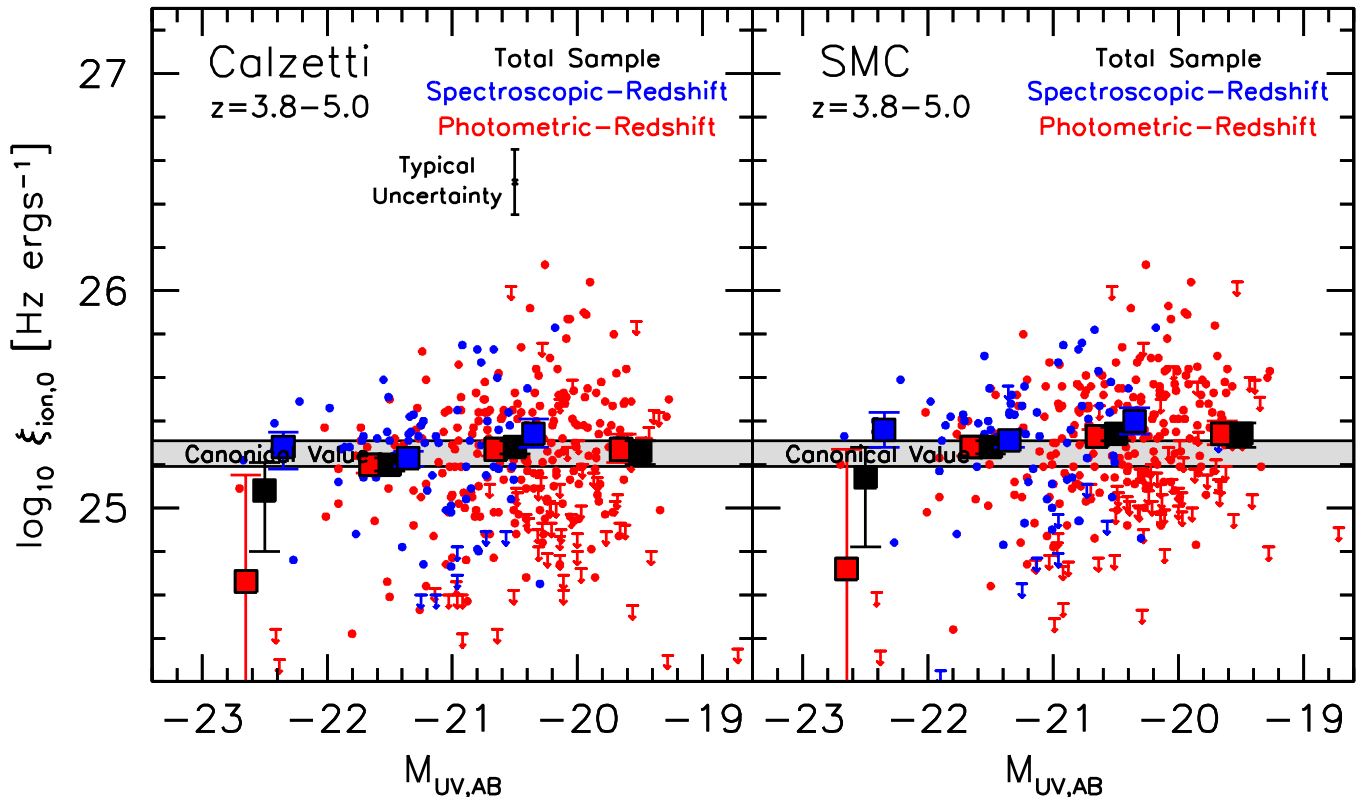


FIG. 1.— Derived Lyman-continuum photon production efficiencies ξ_{ion} based on the $H\alpha$ luminosities derived from a fit to the IRAC fluxes in $z \sim 4-5$ galaxies and assuming a Calzetti et al. (2000: *left panel*) or SMC-like dust law (*right panel*: §3.2). A Lyman-continuum escape fraction of zero has been assumed in deriving these $\xi_{ion,0}$'s (see §3.5 for the values with non-zero escape fractions). Sources where spectroscopic redshifts or well-determined photometric redshifts place the $H\alpha$ line in a specific IRAC band are indicated by the blue and red points, respectively. 1σ upper limits are included on this diagram with downward arrows in cases where the $H\alpha$ emission line is not detected at 1σ in the photometry. The solid red and blue squares indicate the mean value of ξ_{ion} for red and blue colored points, while the solid black square indicates the mean values combining the spectroscopic and photometric-redshift selected samples (shown for all bins with >1 source and offset from the center of the bin for clarity). The grey band indicates the Lyman-continuum photon production efficiencies ξ_{ion} assumed in typical models (Table 2). The black error bar near the top of the left panel indicate the typical uncertainties in the derived ξ_{ion} 's. The ξ_{ion} values we observe for both dust laws are consistent with the values assumed in canonical reionization models; however, we note a slight preference for higher ξ_{ion} 's adopting the SMC dust law.

This procedure leads to an estimate of the flux in the $H\alpha$ line and other lines at approximately the same wavelength. One such line is [NII], but other lines (e.g., [SII]) also contribute. As in Smit et al. (2015b) and Rasappu et al. (2015), we estimate the impact of the [NII] emission line on the measured $H\alpha$ flux based on the model results of Anders & Fritze-v. Alvensleben (2003), where [NII]/ $H\alpha$ is 6.8% and [SII]/ $H\alpha$ is 9.5%. These line ratios are very consistent with that found for normal to lower-mass galaxies at $z = 2.9-3.8$ galaxies (e.g., Sanders et al. 2014). We verified that the model SED fits for all sources used in our study were sufficiently good as to produce credible measurement of $L_{H\alpha}$, and no sources from Smit et al. (2016) were excluded.

The present methodology is almost identical to the methodology employed in Shim et al. (2011), Stark et al. (2013), and most recently Marmol-Queralto et al. (2015). While one might be concerned that this approach may lead to small systematic errors in the fluxes in various emission lines, one can test the accuracy of the flux measurements by comparing the [3.6]–[4.5] colors of $3.1 < z < 3.6$, $z = 3.8-5.0$, and $z = 5.1-5.4$ galaxy samples. Encouragingly enough, the estimated EWs one derives from differential comparisons of the [3.6]–[4.5] colors agree very well with the fit results performed on

the individual SEDs. For example, in Rasappu et al. (2015: comparing $z = 4.4-5.0$ and $z = 5.1-5.4$ samples), the mean $H\alpha$ EW we derive from the SED fits for the photometric samples is $638 \pm 118 \text{ \AA}$ (vs. $665 \pm 53 \text{ \AA}$ from the differential comparison) and $855 \pm 179 \text{ \AA}$ for the spectroscopic samples (vs. $707 \pm 74 \text{ \AA}$ from the differential comparison). Marmol-Queralto et al. (2015) also demonstrate that they achieve equivalent constraints on the $H\alpha + [NII]$ EWs for $z \sim 1.3$ galaxies using the HST WFC3/IR grism observations from the 3D-HST program (Brammer et al. 2012) as they find using the present SED-fitting procedure.

3.2. Procedure to Derive $\xi_{ion,0}$

The intrinsic $H\alpha$ luminosity from a galaxy is closely connected to its total Lyman-continuum luminosity. Based on the simulations of Leitherer & Heckman (1995) and assuming an escape fraction of zero for Lyman-continuum photons into the intergalactic medium, the $H\alpha$ luminosity $L(H\alpha)$ can be expressed in terms of the production rate of Lyman-continuum photons $N(H^0)$, as

$$L(H\alpha)[\text{ergs s}^{-1}] = 1.36 \times 10^{-12} N(H^0)[\text{s}^{-1}] \quad (1)$$

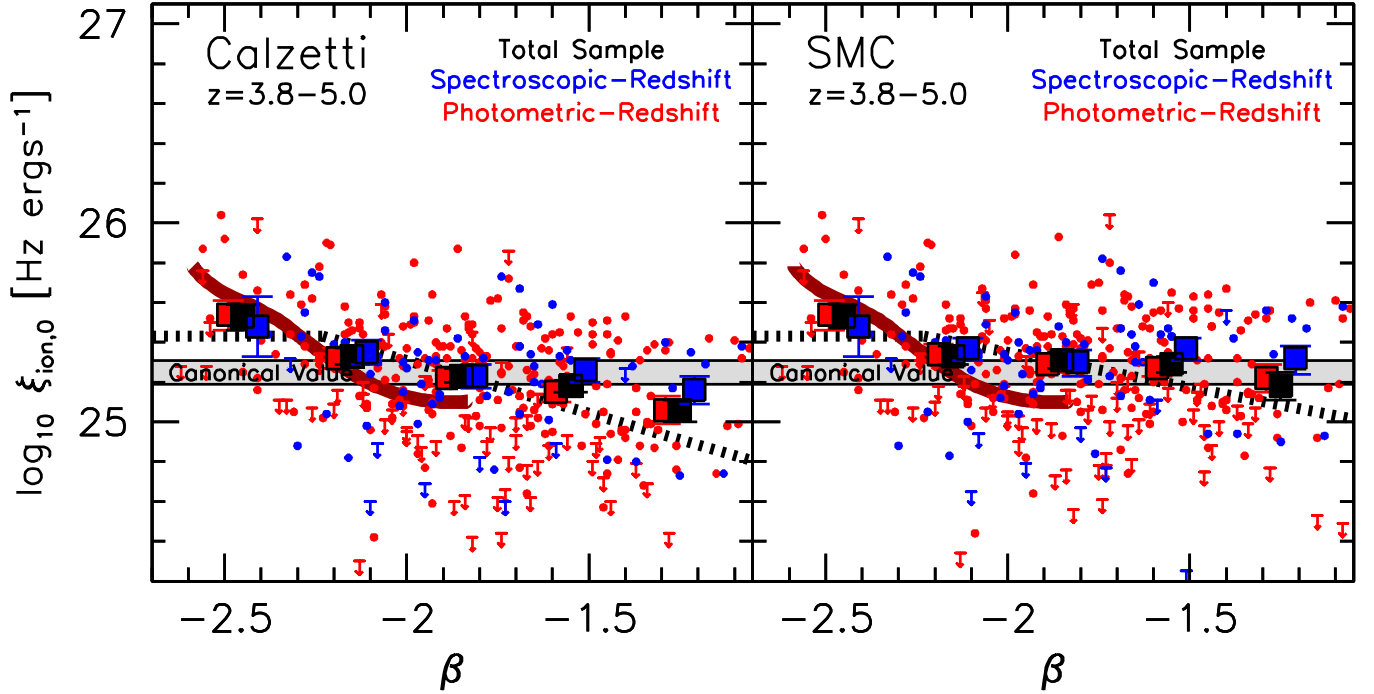


FIG. 2.— Dependence on ξ_{ion} 's we have derived on the UV -continuum slope β assuming either a Calzetti et al. (2000) extinction law (left panel) or a SMC-like extinction law (right panel: §3.2). A Lyman-continuum escape fraction of zero has been assumed in deriving these $\xi_{ion,0}$'s (see §3.5 for the values with non-zero escape fractions). The red, blue, and black symbols are the same as on Figure 1. The thick dotted lines show the trend in $\xi_{ion,0}$ vs. β that would result from the impact of dust corrections on the observed IRAC excesses and UV magnitudes. The thick red line indicates the predicted ξ_{ion} vs. β trend for a stellar population model with zero dust extinction, a metallicity of $0.4Z_{\odot}$, and a range in ages using the Bruzual & Charlot (2003) models (see Robertson et al. 2013; Duncan & Conselice 2015; Bouwens et al. 2015b). Independent of our assumptions about the dust law, we consistently derive higher values for ξ_{ion} (by ~ 0.2 dex) for the bluest galaxies than have been canonically assumed for the star-forming population as a whole (but consistent with the higher values suggested by Duncan & Conselice 2015 and Bouwens et al. 2015b for the bluest galaxies). Our ξ_{ion} results for both dust laws are consistent with canonically assumed values. We note a slight preference for higher values (by ~ 0.1 dex) of ξ_{ion} adopting the SMC dust law.

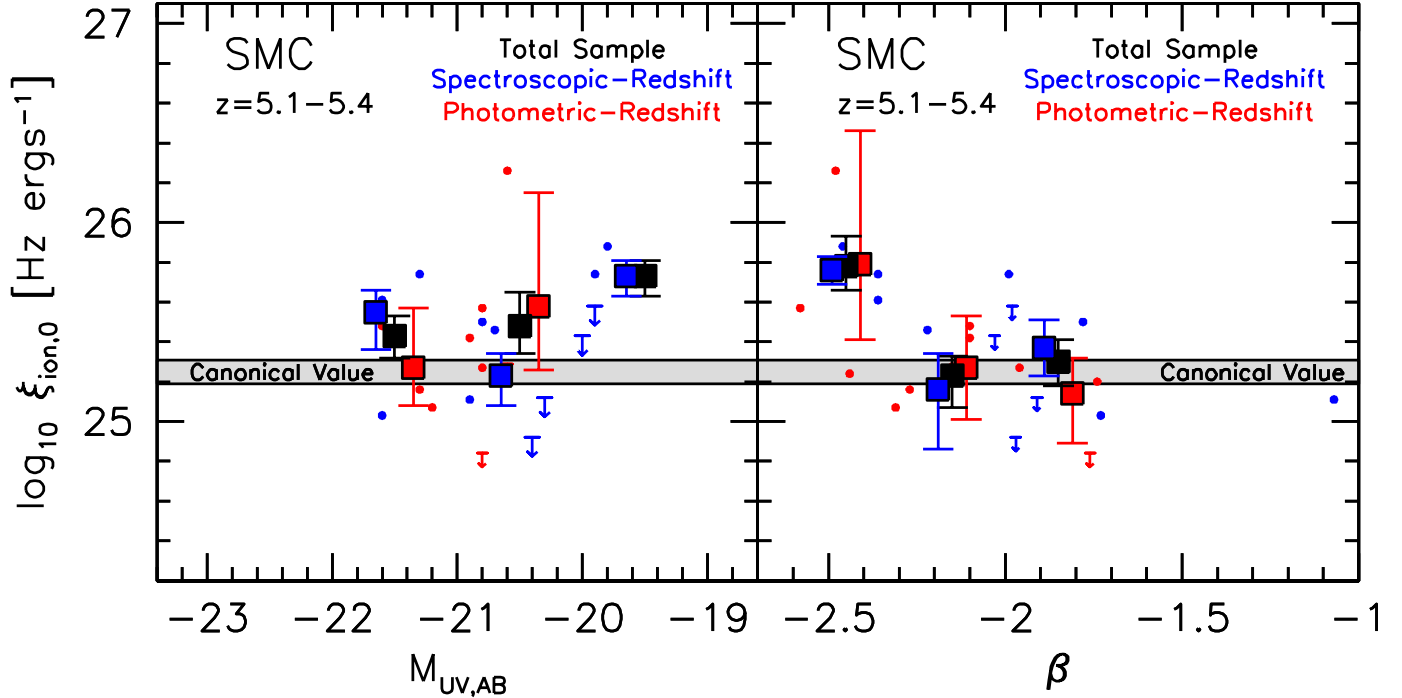


FIG. 3.— The ξ_{ion} 's we have derived assuming the SMC dust law for $z = 5.1-5.4$ galaxies from the Rasappu et al. (2015) selection shown as a function of their UV luminosity and UV -continuum slope β (§3.2). The blue, red, and black symbols are the same as on Figure 1. As in Figure 2, we find that the bluest sources show particularly elevated values of ξ_{ion} relative to canonically-assumed values.

An essentially identical conversion factor is quoted in many other places (e.g., Kennicutt 1983, 1998; Gallagher et al. 1984). The above relationship is known to be slightly temperature and metallicity dependent (e.g., Charlot & Longhetti 2001). However, in general, these dependencies are much smaller than in converting either of these quantities to other quantities like the star formation rate. Overall, the uncertainties are not expected to be larger than 15% (0.06 dex).

It is worthwhile noting that we can make use of Eq. 1 even in cases where a small fraction of Lyman-continuum photons do escape; we simply need to reinterpret $N(\text{H}^0)$ as referring to those photons that do not escape from galaxies.

To make use of Eq. 1 to derive the production rate of Lyman-continuum photons $N(\text{H}^0)$ for all sources, we need to correct the apparent $\text{H}\alpha$ fluxes we observe for the impact of dust extinction. For our baseline results, we derive the estimated extinction based on the measured UV -continuum slopes β for individual sources, assuming a Calzetti et al. (2000) extinction law (adopting the relation $A_{UV} = 1.99(\beta + 2.23)$; Meurer et al. 1999), and assuming similar extinction for the nebular lines, as for the continuum starlight. Shivaeei et al. (2015) demonstrated that such a prescription produced reasonable agreement between the inferred SFRs in the UV , $\text{H}\alpha$, and mid-IR (from MIPS) inferred for galaxies at $z \sim 2$. The β 's we utilize for our dust corrections are derived from power-law fits to the observed fluxes (where $f_\lambda \propto \lambda^\beta$), as was first done in the works of Bouwens et al. (2012b) and Castellano et al. (2012). For sources where $\beta < -2.23$ (where $A_{UV} = 0$ according to the Calzetti et al. (2000) dust law), we take the dust correction to be zero.

We have made use of Eq. 1 to derive the production rate of Lyman-continuum photons $N(\text{H}^0)$ for all sources in our samples. We can then calculate the Lyman-continuum photon production efficiency $\xi_{ion,0}$ as follows (with a zero subscript to indicate that an escape fraction of zero is assumed for ionizing photons):

$$\xi_{ion,0} = \frac{N(\text{H}^0)}{L_{UV}/f_{esc,UV}} \quad (2)$$

where L_{UV} is the UV -continuum luminosity observed for various individual sources and $1/f_{esc,UV}$ is the dust correction to convert the observed luminosity of a source in the UV -continuum to the intrinsic luminosity (prior to the impact of dust).

3.3. $\xi_{ion,0}$ vs. M_{UV} and β

We have presented the resultant $\xi_{ion,0}$'s for individual sources in Figures 1 and 2 (*left panels*) as a function of the UV luminosities M_{UV} of individual sources and also the UV -continuum slopes β 's for sources in our $z = 3.8$ -5.0 sample. In Figure 1 and 2, we present separately the results from our spectroscopic and photometric redshift selections, as well as the results from our total sample. In the same figures, the mean $\xi_{ion,0}$ we have derived for sources is also shown as a function of both UV luminosity M_{UV} and β . The same results are also presented in Table 1.

Observational uncertainties in β can impact the mean $\xi_{ion,0}$ vs. β relationship we infer through dust corrections

we apply (as we show with the thick dotted lines on Figure 2). To determine the impact of errors in β on our result, we repeated our determination of $\xi_{ion,0}$ in each β bin 300 times, but scattering the determined β 's by a $\sigma(\beta)$ of 0.2. [$\sigma(\beta) \sim 0.2$ is the observational uncertainty at $z \sim 4$ and $z \sim 5$ for sources in the luminosity range we consider (Appendix B.3 of Bouwens et al. 2012b).] None of the derived $\xi_{ion,0}$'s changed by >0.05 dex as a result of adding a small scatter to β . We applied this small correction to the $\xi_{ion,0}$ values we report in Figure 2 and Table 1.

Given the formal size of the statistical errors on the mean $\xi_{ion,0}$ values we derive, i.e., 0.02-0.04 dex, for different subsamples, systematic errors likely contribute meaningfully to the overall error budget. Nevertheless, given the consistency of the median $\text{H}\alpha$ equivalent width measurements derived from fitting to the SEDs of individual sources and that derived from comparisons of the [3.6] – [4.5] colors for different redshift subsamples (see §3.1), systematic errors on ξ_{ion} seem likely to be modest. We can estimate the size by comparing the median [3.6] excess derived by Stark et al. (2013) using these two difference approaches, i.e., 0.37 and 0.33 mag. The two different measures of the excess translate to $\text{H}\alpha$ luminosities that differ at the 0.06 dex level. We adopt 0.06 dex as our fiducial estimate of the systematic error in ξ_{ion} .

For sources with redder β 's, our $\xi_{ion,0}$ results are in good agreement with the canonical values (Table 2). However, we derive particularly elevated $\xi_{ion,0}$'s (0.2 dex higher than canonical assumed values) for $z = 3.8$ -5.0 galaxies with the bluest UV -continuum slopes β ($\beta < -2.3$). Higher values of ξ_{ion} have indeed been predicted for those galaxies with the bluest slopes (Bouwens et al. 2015b; Duncan & Conselice 2015), so it is encouraging that our measurements provide empirical support for these particularly elevated values of ξ_{ion} . It is worthwhile noting that this result remains the case, regardless of what one assumes about the dust law.

Given that many early ALMA results appear to be suggesting that the typical $z \sim 5$ -6 galaxy exhibits more of an SMC extinction law (e.g., Capak et al. 2015) than a Calzetti et al. (2000) extinction law, we also utilize the SMC dust law to correct the apparent $\text{H}\alpha$ and UV -continuum fluxes and derive Lyman-continuum photon production efficiencies $\xi_{ion,0}$ (adopting the relation $A_{UV} = 1.1(\beta + 2.23)$ while again assuming an escape fraction of zero for ionizing photons).⁵ Our results are presented in the right panels of Figures 1 and 2. Interestingly enough, the $\xi_{ion,0}$'s we derive for the SMC extinction law are ~ 0.07 dex higher than Calzetti and ~ 0.1 dex higher than some canonically assumed values (e.g., Robertson et al. 2015). We discuss comparisons with previous estimates more extensively in §3.6.

It also makes sense for us to also derive $\xi_{ion,0}$ for the Rasappu et al. (2015) $z = 5.1$ -5.4 samples. We present the results in Figure 3 using the SMC extinction law. Overall, the results are in reasonable agreement with those from the Smit et al. (2015b) $z = 3.8$ -5.0 sample. One other striking similarity to the $z = 3.8$ -5.0 results is that the bluest ($\beta < -2.3$) sources show particularly

⁵ We have derived the extinction relation $A_{UV} = 1.1(\beta + 2.23)$ from the SMC observations and results from Prevot et al. (1984), Bouchet et al. (1985), and Lequeux et al. (1982).

TABLE 1
THE MEAN $\xi_{ion,0}$ 'S WE DERIVE FROM THE INFERRED H α FLUX
FOR GALAXIES OF DIFFERENT LUMINOSITIES AND
UV-CONTINUUM SLOPES β .

| Subsample | # Sources | $\log_{10} \xi_{ion,0} / [\text{Hz ergs}^{-1}]^a$ | |
|---|-----------|---|-------------------------|
| | | Calzetti | SMC |
| <i>z</i> = 3.8-5.0 Sample (Smit et al. 2015b) | | | |
| $-2.6 < \beta < -2.3$ | 25 | $25.53^{+0.05}_{-0.07}$ | $25.53^{+0.06}_{-0.06}$ |
| $-2.3 < \beta < -2.0$ | 71 | $25.33^{+0.04}_{-0.04}$ | $25.34^{+0.04}_{-0.04}$ |
| $-2.0 < \beta < -1.7$ | 96 | $25.23^{+0.04}_{-0.05}$ | $25.30^{+0.04}_{-0.04}$ |
| $-1.7 < \beta < -1.4$ | 88 | $25.18^{+0.03}_{-0.04}$ | $25.29^{+0.03}_{-0.04}$ |
| $-1.4 < \beta < -1.1$ | 32 | $25.06^{+0.05}_{-0.05}$ | $25.22^{+0.05}_{-0.05}$ |
| $-23.0 < M_{UV} < -22.0$ | 9 | $25.08^{+0.14}_{-0.33}$ | $25.14^{+0.14}_{-0.26}$ |
| $-22.0 < M_{UV} < -21.0$ | 64 | $25.20^{+0.03}_{-0.03}$ | $25.28^{+0.03}_{-0.03}$ |
| $-21.0 < M_{UV} < -20.0$ | 195 | $25.28^{+0.03}_{-0.03}$ | $25.34^{+0.03}_{-0.03}$ |
| $-20.0 < M_{UV} < -19.0$ | 68 | $25.26^{+0.05}_{-0.06}$ | $25.34^{+0.05}_{-0.06}$ |
| <i>z</i> = 5.1-5.4 Sample (Rasappu et al. 2015) | | | |
| $-2.6 < \beta < -2.3$ | 7 | — | $25.78^{+0.15}_{-0.12}$ |
| $-2.3 < \beta < -2.0$ | 6 | — | $25.23^{+0.10}_{-0.16}$ |
| $-2.0 < \beta < -1.7$ | 9 | — | $25.30^{+0.12}_{-0.11}$ |
| $-22.0 < M_{UV} < -21.0$ | 6 | — | $25.43^{+0.10}_{-0.11}$ |
| $-21.0 < M_{UV} < -20.0$ | 13 | — | $25.48^{+0.17}_{-0.14}$ |
| $-20.0 < M_{UV} < -19.0$ | 3 | — | $25.73^{+0.08}_{-0.10}$ |

^a Assumes that the escape fraction is zero. The estimated $\xi_{ion,0}$'s would be ~ 0.03 dex higher if we account for a positive escape fraction and suppose that galaxies dominate the observed ionizing emissivity at $z \sim 4-5$. See §3.5. In addition to the formal uncertainties quoted on ξ_{ion} , the derived values are likely subject to a small systematic error, i.e., 0.06 dex (see §3.3).

elevated values of $\xi_{ion,0}$, again lying ~ 0.25 dex above the canonical relationship.

Focusing on the sub-L* (> -21 mag) sources that likely play the dominant role in reionizing the universe (e.g., Yan & Windhorst 2004; Bouwens et al. 2006, 2007, 2011; Oesch et al. 2010; Robertson et al. 2013), we find a mean $\log_{10} \xi_{ion,0} / [\text{Hz ergs}^{-1}]$ of $25.27^{+0.03}_{-0.03}$ and $25.34^{+0.02}_{-0.02}$ for the Smit et al. (2015b) $z = 3.8-5.0$ sample based on the Calzetti and SMC extinction laws, respectively. For the Rasappu et al. (2015) $z = 5.1-5.4$ sample, we find $25.51^{+0.12}_{-0.12}$ and $25.54^{+0.12}_{-0.12}$, respectively, for the same two extinction laws. We emphasize that the values we derive here do not account for a non-zero escape fraction. We derive larger production efficiencies (§3.5) accounting for a positive escape fraction.

We infer ~ 0.3 dex intrinsic scatter in the values of ξ_{ion} at a given luminosity. In the luminosity range $-21 < M_{UV,AB} < -20$, we measure a scatter of ~ 0.31 dex. If one accounts for the fact that the observational uncertainty in ξ_{ion} is estimated to be ~ 0.18 , this translates into an intrinsic scatter of ~ 0.25 dex, very similar to the observed scatter in the main sequence of star formation in galaxies, as inferred from H α (Smit et al. 2015b). See Figure 4. A 0.25 dex intrinsic scatter is estimated in ξ_{ion} from a simple modeling of the fraction of sources lying above a given observed value of ξ_{ion} and accounting for noise in the individual measurements of ξ_{ion} .

3.4. Dust Extinction Impacting the Nebular vs. Stellar Continuum Light

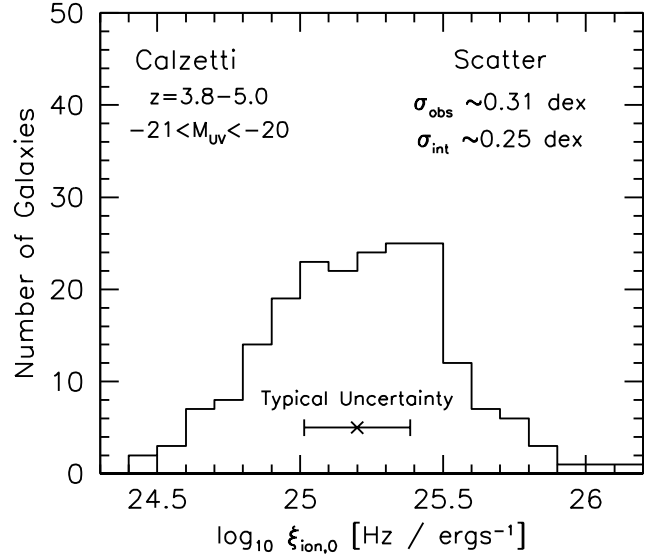


FIG. 4.— Distribution of ξ_{ion} 's estimated from the observations for $z = 3.8-5.0$ galaxies in the luminosity range $-21 < M_{UV,AB} < -20$ assuming a Calzetti dust law. For 10% of the sources where H α is not detected at 1σ significance, the individual ξ_{ion} values are presented at their 1σ upper limits on the histogram. The observed scatter in this distribution is ~ 0.31 dex. Given that the typical uncertainty in individual estimates of ξ_{ion} is ~ 0.18 dex (shown as a horizontal error bar with respect to the median ξ_{ion} plotted as a cross), this implies an intrinsic scatter of ~ 0.25 dex, very similar to the scatter around the main sequence of star formation in galaxies, as estimated by Smit et al. (2015b) based on the inferred H α fluxes. Essentially an identical intrinsic scatter is derived modeling the cumulative distribution of ξ_{ion} values accounting for individual observational errors. See §3.3.

In addition to uncertainties that directly regard the dust law, it is also unclear whether emission lines suffer more extinction than stellar continuum light due to a significant dust mass in nebular regions of galaxies. While the nebular continuum is known to be more extinguished than the stellar continuum in the local universe, i.e., $A_{V,stellar} = 0.44A_{V,gas}$ (Calzetti et al. 1997, 2000), select results at $z \sim 2$ suggests that this is not true for all $z \sim 2$ galaxies and many exhibit $A_{V,stellar} = A_{V,gas}$ (e.g., Erb et al. 2006; Reddy et al. 2010, 2015; but see also Förster Schreiber et al. 2009; Kashino et al. 2013; Price et al. 2014).

We rederived $\xi_{ion,0}$ for the individual sources in our samples assuming that nebular lines suffer a $2.3\times$ higher dust obscuration. In this case, the derived $\xi_{ion,0}$ would be 0.09 dex and 0.02 dex higher for the Calzetti and SMC dust laws, respectively. We do not correct our baseline determinations for this effect given evidence from other studies (e.g., Shivaee et al. 2015) that such a correction is not clearly necessary for achieving agreement between UV, H α , and mid-IR-based SFR estimates.

3.5. Sensitivity to the Assumed Escape Fraction

A separate factor which impacts the Lyman-continuum photon production efficiency ξ_{ion} is the escape fraction of ionizing photons we assume. If the escape fraction is larger than zero, then some fraction of the ionizing photons are escaping from a galaxy without having an impact on the number of ionized hydrogen atoms within a galaxy and also on its H α luminosity. The implication

is that those photons which do not escape must be even more rich in Lyman-continuum photons (per unit UV luminosity) than we would infer if no radiation at all was escaping.

Following the work of Kuhlen & Faucher-Giguère (2012), we can set upper limits on the escape fraction of ionizing radiation at $z \sim 4.4$ from galaxies by comparing the UV luminosity density integrated to various limiting luminosities with measurements of the ionizing emissivity \dot{N}_{ion} . The relevant equation is

$$\dot{N}_{ion} = f_{esc} \xi_{ion} \rho_{UV} \quad (3)$$

(e.g., Robertson et al. 2013; see also Kuhlen & Faucher-Giguère 2012). The ionizing emissivity has been measured at $z \sim 4.4$ based on observations of the Lyman- α forest which constrain both the ionizing background and the mean-free path of ionizing photons; interpolating between the $z \sim 4$ and $z \sim 4.75$ measurements of Becker & Bolton (2013), we adopt a value of $10^{50.92 \pm 0.45} \text{ s}^{-1} \text{ Mpc}^{-3}$. If we assume that the UV LF has a faint-end cut-off at -13 mag, then the integrated luminosity we estimate by interpolating between the $z \sim 3.8$ and $z \sim 4.9$ LF results from Bouwens et al. (2015a) is $10^{26.56 \pm 0.06} \text{ ergs s}^{-1} \text{ Hz}^{-1} \text{ Mpc}^{-3}$. ξ_{ion} represents the Lyman-continuum photon production efficiency in the presence of a non-zero escape fraction and is equal to $\xi_{ion,0}/(1 - f_{esc,LyC})$. Meanwhile, f_{esc} represents the so-called relative escape fraction $f_{esc} = f_{esc,LyC}/f_{esc,UV}$ where $f_{esc,LyC}$ and $f_{esc,UV}$ represent the escape fraction at Lyman-continuum and UV -continuum wavelengths, respectively (see e.g. Steidel et al. 2001; Shapley et al. 2006; Siana et al. 2010). The expanded expression is $f_{esc,LyC} \xi_{ion,0}/(1 - f_{esc,LyC})/f_{esc,UV} = \dot{N}_{ion}/\rho_{UV}$ if galaxies provide the dominant contribution to the ionizing emissivity at $z = 4-5$.

If we consider the case that $\beta \sim -2$ (which is typical for sources in the magnitude range we consider: Bouwens et al. 2014), the escape fraction of UV -continuum photons $f_{esc,UV}$ is 0.8 adopting the SMC dust extinction law (where $\log_{10} \xi_{ion,0}/[\text{Hz ergs}^{-1}] = 25.34$). This translates to $f_{esc,LyC}$ being equal to $0.08^{+0.12}_{-0.05}$. The quoted errors here allow for the full range of systematic errors permitted in the ionizing emissivity results of Becker & Bolton (2013). If the dust curve is Calzetti and $f_{esc,UV} = 0.7$ for a $\beta \sim -2$ source, then $f_{esc,LyC} = 0.08^{+0.12}_{-0.05}$.

These estimated escape fractions imply that ξ_{ion} can be at most $\log_{10} 1/(1 - 0.08^{+0.12}_{-0.05}) \sim 0.03^{+0.06}_{-0.02}$ dex larger than what we measure for $\xi_{ion,0}$ from the inferred $H\alpha$ fluxes.

3.6. Comparison with Previous Estimates

The literature is full of a wide variety of observational, theoretical, and empirical results for the Lyman-continuum photon production efficiency ξ_{ion} . Table 2 provides a useful summary of many of them.

3.6.1. Suggested Values from Stellar Population Models

Many of the first estimates were based on the results of standard stellar population models (e.g., Bruzual & Charlot 2003) at normal or slightly sub-solar metallicities (Madau et al. 1999; Bouwens et al. 2012a; Kuhlen & Faucher-Giguère 2012; Finkelstein et al. 2012b). Many

TABLE 2
CURRENT MEASUREMENTS OF $\xi_{ion,0}$ VS. THOSE
PREVIOUSLY ASSUMED IN REIONIZATION MODELS.

| Empirical Determination | $\log_{10} \xi_{ion,0}$ [Hz ergs $^{-1}$] |
|---|---|
| Current Determinations | |
| $z = 3.8-5.0$ | |
| Fiducial Determination (SMC Dust) ^{a,†} | $25.34^{+0.02}_{-0.02} \text{ b,†}$ |
| Calzetti Dust Extinction ^{a,†} | $25.27^{+0.03}_{-0.03} \text{ b,†}$ |
| $z = 5.1-5.4$ | |
| Fiducial Determination (SMC Dust) ^{a,†} | $25.54^{+0.12}_{-0.12} \text{ b,†}$ |
| Calzetti Dust Extinction ^{a,†} | $25.51^{+0.12}_{-0.12} \text{ b,†}$ |
| Previous Estimates | |
| $z = 7.045$: Stark et al. (2015) | |
| | $25.68^{+0.27}_{-0.19} \text{ c}$ |
| Based on Previously Inferred $L_{H\alpha}$ and SFR_{UV} Values | |
| $z \sim 4.5$: Shim et al. (2011) | |
| | $25.72^{+0.04}_{-0.04} \text{ e,†}$ |
| $z \sim 4.5$: Marmol-Queralto et al. (2016) | |
| | $25.08^{+0.04}_{-0.04} \text{ f,†}$ |
| Based on Canonical Conversion Factors | |
| Kennicutt (1998) ^d | |
| | 25.11 |
| Previously Suggested Values | |
| Madau et al. (1999) | |
| | 25.3 |
| Robertson et al. (2013) | |
| | 25.20 |
| Robertson et al. (2015) | |
| | 25.24 |
| Topping & Shull (2015) | |
| | $25.4 \pm 0.2^{\text{g}}$ |
| Bouwens et al. (2015b,c) | |
| | 25.46 |
| Kuhlen & Faucher-Giguère (2012) | |
| | 25.30 |
| | 25.00 - 25.60 |
| Bouwens et al. (2012a) | |
| | 25.30 |
| Finkelstein et al. (2012b) | |
| | 25.28^{h} |
| Duncan & Conselice (2015) Model A | |
| | 25.18 |

[†] In addition to the formal uncertainties quoted on ξ_{ion} , the derived values are likely subject to a small systematic error, i.e., 0.06 dex (see §3.3).

^a $E(B - V)_{neb} = E(B - V)_{stellar}$

^b If we assume that galaxies provide the dominant contribution to the cosmic ionizing emissivity at $z > 4$, we require a non-zero Lyman-continuum escape fraction from galaxies. If we account for this, the ξ_{ion} 's we derive would be 0.03 dex higher (§3.5).

^c Constraints on ξ_{ion} using the detected flux in the CIV λ 1548 emission line.

^d Implied value of ξ_{ion} using the conversion factors Kennicutt (1998) quote for converting UV and $H\alpha$ luminosities into star formation rates.

^e Implied value of ξ_{ion} based on the median UV to $H\alpha$ SFRs quoted by Shim et al. (2011). As Shim et al. (2011) consider those sources with significant evidence for $H\alpha$ emission, their ξ_{ion} might be expected to be significantly higher than what we derive.

^f Implied value of ξ_{ion} based on the median UV to $H\alpha$ SFRs quoted by Marmol-Queralto et al. (2016). Using our own results, we estimate this value to be lower than our own fiducial determination using a sub- L^* sample, since this value is the median rather than the mean (impact of 0.08 dex) and is derived using a high-mass ($>10^{9.5} M_{\odot}$) subsample (impact of 0.08 dex).

^g Converted using Salpeter IMF

^h At face value, the 13% factor advocated here is similar to values suggested in previous work (Finkelstein et al. 2012b), but the correspondence is accidental given significant changes in the preferred values for both $\dot{N}_{ion}(z = 6)$ and ξ_{ion} (as well as ρ_{UV}) over the last three years. Of particular note, Bouwens et al. (2015b) have presented evidence based on a simple modeling of the ionizing emissivity evolution that $\dot{N}_{ion}(z = 6)$ is likely $\sim 0.3-0.5$ dex higher than concluded by Bolton & Haehnelt (2007) using more direct methods.

relevant models (Schaerer 2003; see also Bruzual & Charlot 2003) suggested $\log_{10} \xi_{ion}/[\text{Hz ergs}^{-1}]$ values of 25.20 at solar metallicities.

Use of the conversion factors from Kennicutt (1998) indicate 25.11 for the value of $\log_{10} \xi_{ion}/[\text{Hz ergs}^{-1}]$.

3.6.2. Inferred from the Measured UV-continuum Slopes

ξ_{ion} has also been estimated based on the mean UV-continuum slopes β derived in a number of different observational studies (Robertson et al. 2013, 2015; Bouwens et al. 2015b; Duncan & Conselice 2015). Robertson et al. (2013) attempted to match $\beta \sim -2$ measurements by Dunlop et al. (2013) and estimated $\log_{10} \xi_{ion}/[\text{Hz ergs}^{-1}]$ to be 25.20.

Meanwhile, Bouwens et al. (2015b) found $\log_{10} \xi_{ion}/[\text{Hz ergs}^{-1}]$ to be 25.46 using a similar procedure to Robertson et al. (2013) but with aim of matching the mean β value of ~ -2.3 derived by Bouwens et al. (2014) for fainter $z \sim 7$ galaxies. Duncan & Conselice (2015) also made note of the bluer β values derived for fainter galaxies by Bouwens et al. (2012b), Bouwens et al. (2014), Rogers et al. (2014), and Finkelstein et al. (2012a) and also the bluer β 's derived for galaxies at higher redshifts (Bouwens et al. 2012b, 2014; Finkelstein et al. 2012a; Hathi et al. 2013; Kurczynski et al. 2014; see also Wilkins et al. 2015).

3.6.3. From near-UV Spectroscopy

Another recent estimate of the Lyman-continuum photon production efficiency $\log_{10} \xi_{ion}/[\text{Hz ergs}^{-1}]$ is $\log_{10} \xi_{ion}/[\text{Hz ergs}^{-1}] = 25.68^{+0.27}_{-0.19}$ and came from a recent analysis by Stark et al. (2015) of a lensed $z = 7.045$ galaxy A1703-zD6 behind Abell 1703 (Bradley et al. 2012). Stark et al. (2015) obtained this result from an analysis of the near-infrared spectrum they collected of this source, which excitedly enough shows the detection of a prominent CIV λ 1548 emission line. Stark et al. (2015) found they could not reproduce the observed properties of this line, as well as the other properties of the source, without a high production efficiency of Lyman-continuum photons, i.e., $\log_{10} \xi_{ion}/[\text{Hz ergs}^{-1}] = 25.68^{+0.27}_{-0.19}$ and also including photons with energies >20 -30 eV.

While higher than the mean value we obtain for our sample, the $\log_{10} \xi_{ion}$ Stark et al. (2015) derive for this source is actually quite consistent with what we measure for the bluest sources in our selection $25.53^{+0.06}_{-0.06}$ (Table 1), especially considering the intrinsic variation in ξ_{ion} that appears to be present across individual sources at $z \sim 4$ -5 (Figure 4). Future spectroscopy on A1703-zD6 probing H α and H β emission with NIRSPEC and MIRI on JWST should provide for an independent test of the $\log_{10} \xi_{ion}/[\text{Hz ergs}^{-1}]$ measured by Stark et al. (2015).

3.6.4. Based on Previous $L_{H\alpha}$ Measurements

Previous work even provide implicit determinations of the Lyman-continuum photon production efficiency ξ_{ion} for $z \sim 4$ -5 galaxies based on the inferred H α and UV luminosities, even though it was specifically represented in these terms.

One such study is from Shim et al. (2011). Shim et al. (2011) provide H α luminosities $L_{H\alpha}$ and UV-based SFRs

TABLE 3
REQUIRED VALUES OF f_{esc} FOR DIFFERENT M_{lim} AND CLUMPING FACTORS C_{HII} ASSUMING THAT GALAXIES DRIVE THE REIONIZATION OF THE UNIVERSE.^a

| C_{HII} | Required f_{esc} ($= f_{esc,LyC}/f_{esc,UV}$) $\xi_{ion} = 10^{25.37 \dagger} \text{ Hz ergs}^{-1}$ | | |
|------------------|--|------------------------|------------------------|
| | $M_{lim} = -17$ | $M_{lim} = -13$ | $M_{lim} = -10$ |
| 2.0 | $0.31^{+0.08}_{-0.06}$ | $0.12^{+0.03}_{-0.02}$ | $0.08^{+0.02}_{-0.02}$ |
| 3.0 | $0.35^{+0.09}_{-0.07}$ | $0.13^{+0.03}_{-0.03}$ | $0.09^{+0.02}_{-0.02}$ |
| 5.0 | $0.41^{+0.11}_{-0.09}$ | $0.16^{+0.04}_{-0.03}$ | $0.10^{+0.03}_{-0.02}$ |
| 2.4 [†] | $0.33^{+0.09}_{-0.07}$ | $0.13^{+0.03}_{-0.03}$ | $0.08^{+0.02}_{-0.02}$ |

[†] Redshift Dependence found in the hydrodynamical simulations of Pawlik et al. (2009).

[‡] $10^{25.37} \text{ Hz ergs}^{-1}$ is the approximate Lyman-continuum photon production efficiency ξ_{ion} , if the dust curve is SMC and after accounting for the fact that the ξ_{ion} 's estimated from the inferred H α fluxes do not account for the ~ 9 -10% of the Lyman-continuum photons that escape from galaxies (assuming that galaxies dominate the ionizing emissivity at $z > 4$). See §3.5.

^a These f_{esc} factors can be derived from Eq. (4). Importantly, we can also quote uncertainties on the estimated f_{esc} 's, which follow from the 1σ error estimate (~ 0.1 dex) on the conversion factor $10^{24.50} \text{ Hz ergs}^{-1}$ from UV luminosity density ρ_{UV} to the equivalent ionizing emissivity \dot{N}_{ion} (Bouwens et al. 2015b).

for 74 sources over the GOODS-North and GOODS-South fields with spectroscopic redshifts in the range $z = 3.8$ -5.0. We can compute the equivalent ξ_{ion} from Eq. (2) using their quoted values for $L_{H\alpha}$, SFR_{UV} , and β and converting SFR_{UV} into a UV luminosity using the relations tabulated by Kennicutt (1998). We estimate a value of $25.64^{+0.01}_{-0.04}$ and $25.72^{+0.04}_{-0.04}$ for the median and mean value of $\log_{10} \xi_{ion}/[\text{Hz ergs}^{-1}]$, respectively, assuming an SMC dust law. We would expect the Shim et al. (2011) values to be higher than our values, since they only considered sources which showed clear evidence for an H α emission line in the photometry. The use of such a selection would bias their measured ξ_{ion} towards higher values.

Alternatively, if we make use of the median inferred SFRs from Marmol-Queralto et al. (2016), we find $\log_{10} \xi_{ion}/[\text{Hz ergs}^{-1}]$ to be equal to 25.08, which is lower than what we derive by 0.19 dex. There appear to be two reasons for this difference. First, Marmol-Queralto et al. (2016) quote the median value whereas we quote the mean. Second, Marmol-Queralto et al. (2016) consider a higher-mass subsample, i.e., $> 10^{9.5} M_{\odot}$, than what we consider. If we use our own sample as a guide, these two choices would lower our derived value of $\log_{10} \xi_{ion}/[\text{Hz ergs}^{-1}]$ by 0.08 dex and 0.08 dex, respectively, which when summed essentially match the difference between the two results. See also brief discussion in Smit et al. (2016) regarding the reasonable overall agreement with the Marmol-Queralto et al. (2016) determinations of the H α EWs.

3.7. Redshift Evolution

It is worthwhile investing the apparent evolution of ξ_{ion} with cosmic time. This is shown in Figure 5 for both our mean ξ_{ion} derived from our samples as a whole (*upper panel*) and making exclusive use of sources with the bluest measured β 's, i.e., $\beta < -2.3$ (*lower panel*). Re-

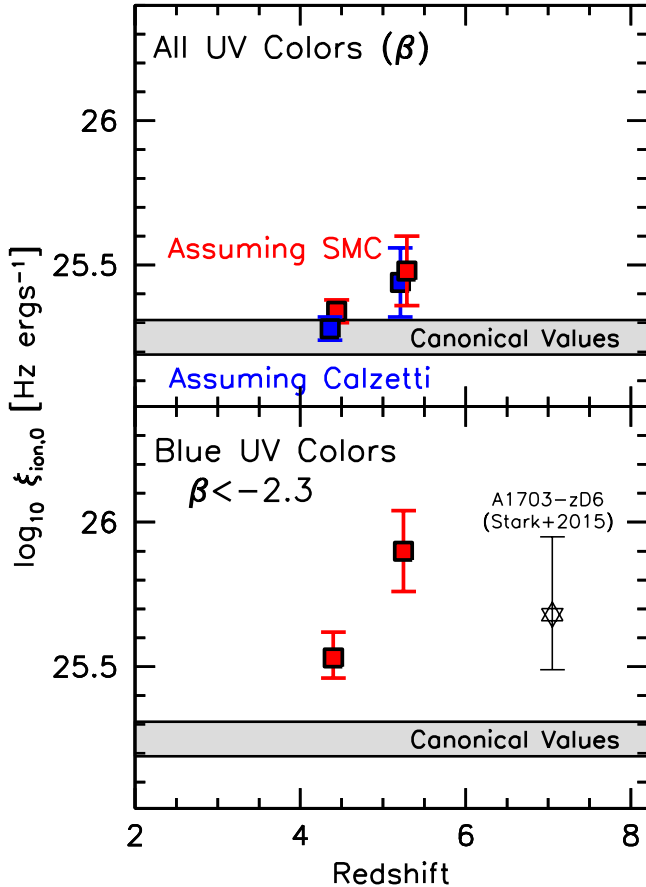


FIG. 5.— (*upper*) Mean Lyman-continuum photon production efficiency ξ_{ion} estimated for star-forming galaxies at $z \sim 4.4$ and $z \sim 5.25$ from the inferred $H\alpha$ flux using both the Calzetti et al. (2000) and SMC dust laws. The plotted values are not corrected for escaping Lyman-continuum photons (if this fraction is significant). Also shown are the canonical ξ_{ion} values utilized in the literature to model the impact of galaxies on the reionization of the universe. Our derived values for ξ_{ion} are either consistent or 1σ higher than canonically assumed values. (*lower*) Mean Lyman-continuum photon production efficiency ξ_{ion} estimated for the bluest ($\beta < -2.3$) star-forming galaxies at $z \sim 4.4$ and $z \sim 5.25$ from the inferred $H\alpha$ flux. Also shown is the ξ_{ion} derived by Stark et al. (2015) for one blue $\beta = -2.4$ $z = 7.045$ galaxy from the observed CIV $\lambda 1548$ line. ξ_{ion} is inferred to be consistently higher (by ~ 0.2 - 0.3 dex) than has been canonically-assumed for the star-formation population as a whole at $z > 6$ in reionization modeling.

sults are presented in assuming both Calzetti and SMC extinction laws. The results are consistent with (or perhaps 1σ higher than) what has been canonically assumed for ξ_{ion} in standard reionization models (e.g., Kuhlen & Faucher-Giguère 2012; Robertson et al. 2013).

Interestingly enough, the ξ_{ion} 's we estimate for the bluest subsample of galaxies are consistently higher than canonically-assumed values, but are consistent with what Stark et al. (2015) estimate for one blue $\beta \sim -2.4$ source at $z = 7.045$. This suggests that those galaxies with the bluest UV colors may be consistently the most efficient at producing the Lyman-continuum photons capable of reionizing the universe.

4. DISCUSSION

In the present work, we have used new measurements of the $H\alpha$ luminosities in $z = 3.8$ - 5.4 galaxies to estimate the Lyman-continuum photon production efficiency

ξ_{ion} . Assuming that early results with ALMA (e.g., Capak et al. 2015) at $z = 5$ - 6 are correct and dust emission is more SMC like, we derive a Lyman-continuum photon production efficiency $\log_{10} \xi_{ion,0}/[\text{Hz ergs}^{-1}]$ of $25.34^{+0.02}_{-0.02}$ at $z = 3.8$ - 5.0 . Higher values (by ~ 0.03 -dex) would be expected if the escape fraction is non-zero and galaxies contribute meaningfully to the observed ionizing emissivity.

Our results for ξ_{ion} are consistent with standard assumptions in canonical models. Nevertheless, for the SMC dust law preferred by early ALMA result, they are suggestive of even higher (~ 0.1 dex) values for ξ_{ion} than traditionally assumed. If the ξ_{ion} values are indeed higher than in canonical modeling, it could have a number of important implications. It would impact our understanding of (1) the stellar populations in $z > 2$ galaxies, (2) the required/allowed escape fraction in high-redshift galaxies, and (3) the methodology for constraining the escape fraction in the future JWST mission.

4.1. Implications for the Stellar Populations of $z > 2$ Galaxies

The present results show that $z > 3$ galaxies produce Lyman-continuum photons at the same rate as (or higher than) expected in conventional stellar population models. In the case that ξ_{ion} is higher than conventional models, we could try to explain this result by adopting particularly bursty star-formation histories for $z > 2$ galaxies.

Such bursty star formation histories are disfavored by several recent results. Specifically, Oesch et al. (2013) find that the $J - [4.5]$ color distribution (providing a measure of the Balmer-break amplitude) shows a generally normal-looking distribution, with a peak at 0.4 mag, which is exactly where one would expect the peak to lie using semi-analytic models based on the Millenium simulations. Secondly, Smit et al. (2015b) find a strong correlation between UV and $H\alpha$ -based specific star formation rates, pointing towards a generally monotonic growth in the SFR and limited variations in the SFR on ~ 10 - 20 Myr time scales.

A more credible explanation for a high production efficiency for Lyman-continuum photons (if confirmed to be the case with smaller uncertainties) would involve evolution in the IMF of galaxies or evolution in the way that high-mass stars evolve at early times. There have been several suggestions that such changes are indeed found in the newer generations of stellar evolution models. It has become clear that massive stars are predominantly found in binaries (Sana et al. 2012) and rotate with a wide range of rotation rates (e.g., Ramirez-Agudelo et al. 2013). The new models that account for these effects predict a higher production efficiency for Lyman-continuum photons at early times when the average metallicity was lower (Yoon et al. 2006; Eldridge & Stanway 2009, 2012; Levesque et al. 2012; de Mink et al. 2013; Kewley et al. 2013; Leitherer et al. 2014; Szécsi et al. 2015; Gräfenner et al. 2015; Stanway et al. 2015).

4.2. Implications for the Escape Fraction

The ξ_{ion} 's we derive from the observations are slightly larger than preferred in some previous work on reionization, particularly in the case of the SMC extinction law, and so it is useful for us to consider the impact this may

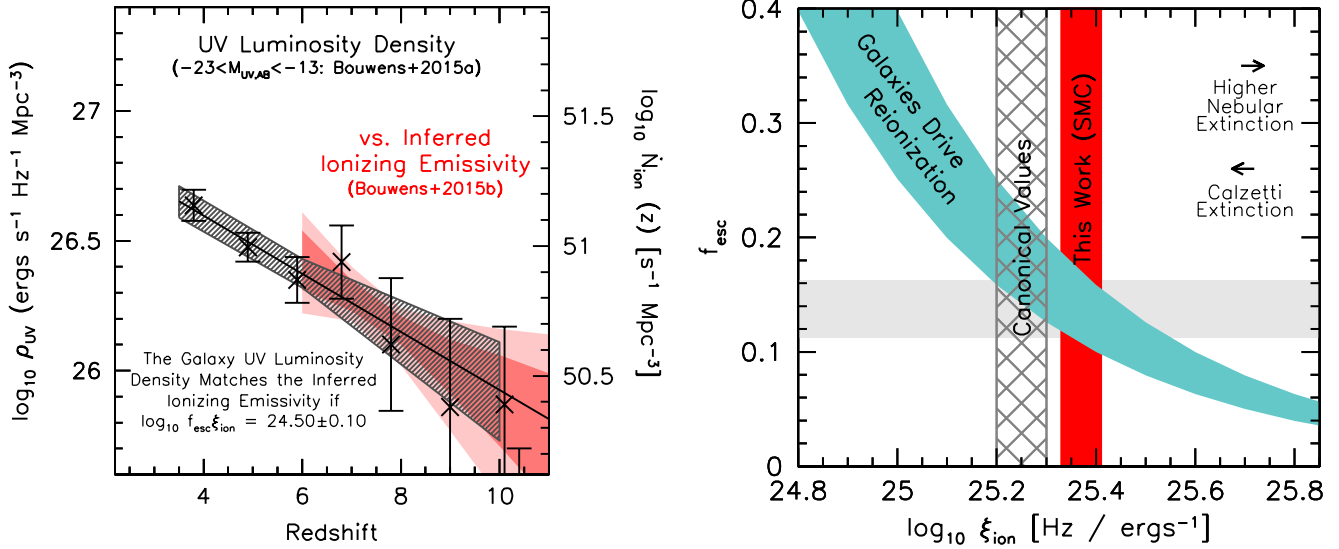


FIG. 6.— Implications from our current ξ_{ion} results for the escape fraction f_{esc} in $z > 6$ galaxies (assuming similar ξ_{ion} 's in $z > 6$ galaxies as at $z = 4-5$). (left) Determinations of the UV luminosity densities at $z = 4-10$ integrated to -13 mag (black crosses with error bars and the shaded regions giving parameterizing fit results: Bouwens et al. 2015b) from several recent LF determinations (Bouwens et al. 2015a; Ishigaki et al. 2015; Oesch et al. 2015) compared to the inferred evolution (dark red and light red contours give the 68% and 95% confidence intervals) of the cosmic ionizing emissivity from $z = 6-12$ (Bouwens et al. 2015b; see also Mitra et al. 2015). As demonstrated first by Robertson et al. (2013, 2015) and later by Bouwens et al. (2015), $\log_{10} f_{esc}\xi_{ion}/[\text{Hz ergs}^{-1}] = 24.50$ if galaxies drive the reionization of the universe, the faint-end cut-off to the LF is -13 , and the clumping factor C is 3; higher values of ξ_{ion} directly translate into lower required values for f_{esc} . (right) Implied constraints on the relative escape fraction $f_{esc} = f_{esc,LyC}/f_{esc,UV}$ for $z \geq 6$ galaxies (horizontal light gray region) that we can set on the basis of our measured ξ_{ion} adopting the relationship $\log_{10} f_{esc}\xi_{ion}/[\text{Hz ergs}^{-1}] = 24.50 \pm 0.10$ (shaded cyan region: §3.5). The dark red regions give the measured ξ_{ion} values our analysis prefers at 68% confidence adopting a SMC extinction law and assuming that galaxies drive the reionization of the universe. If we assume that the dust extinction follows the Calzetti dust law, our measured ξ_{ion} would be 0.07 dex lower; however, if we assume that line emission from nebular regions suffer from more dust extinction than stellar continuum light, our measured ξ_{ion} would be 0.02-0.09 dex higher. The vertical hatched grey region indicates the Lyman-continuum photon production efficiencies ξ_{ion} assumed in typical models (Table 2).

have on the allowed escape fraction for $z > 6$ galaxies, assuming similar ξ_{ion} 's in reionization-era galaxies.

As demonstrated in previous work (e.g., Robertson et al. 2013), we can set strong constraints on the escape fraction f_{esc} if we know ξ_{ion} . [This assumes fiducial choices for other variables, i.e. a clumping factor $C = \langle (n_H)^2 \rangle / \langle n_H \rangle^2$ of 3 and fiducial faint-end cut-off to the LF of -13 .] The implicit constraint in Robertson et al. (2013, 2015) is for $\log_{10} f_{esc}\xi_{ion}/[\text{Hz ergs}^{-1}]$ to equal 24.50. Bouwens et al. (2015) found essentially identical constraints on $f_{esc}\xi_{ion}$ in a follow-up analysis, but presented this constraint in a generalized form to a wider range of faint-end cut-offs to the UV LF M_{lim} and clumping factors C :

$$f_{esc}\xi_{ion}f_{corr}(M_{lim})(C/3)^{-0.3} = 10^{24.50 \pm 0.10} \text{Hz ergs}^{-1} \quad (4)$$

where $f_{corr}(M_{lim}) = 10^{0.02+0.078(M_{lim}+13)-0.0088(M_{lim}+13)^2}$ corrects $\rho_{UV}(z = 8)$ derived to a faint-end limit of $M_{lim} = -13$ mag to account for different M_{lim} 's (left panel of Figure 6).

If we adopt a faint-end cut-off to the UV LF of -13 mag, take the clumping factor C to be 3 (as favored by Pawlik et al. 2009; see also Bolton & Haehnelt 2007, Shull et al. 2012, Finlator et al. 2012; Pawlik et al. 2015) and alternatively take $\log_{10} \xi_{ion}/[\text{Hz ergs}^{-1}]$ to be $25.37^{+0.02}_{-0.03}$ and $25.31^{+0.03}_{-0.03}$ as appropriate for SMC and Calzetti extinction, we estimate f_{esc} to be 0.13 and 0.14, respectively (right panel of Figure 6). Equivalent results

are also presented in Table 3 for other potential clumping factors or faint-end cut-offs to the LF using Eq. 4.

An escape fraction of $\sim 13-14\%$ would be much more consistent with the low fraction of Lyman-continuum, ionizing photons confirmed to be escaping from star-forming galaxies at $z \sim 2-4$. For example, work by Vanzella et al. (2010) and Siana et al. (2015) estimate the escape fraction to be $< 6\%$ and $7-9\%$; meanwhile, analysis of the afterglow spectra for a small sample of gamma-ray bursts (Chen et al. 2007) suggest an escape fraction $f_{esc,rel}$ of $4 \pm 4\%$ at $z \sim 2-4$ (supposing $f_{esc,UV}$ to be ~ 0.5). While many recent estimates of the escape fraction for $z \sim 3$ galaxies yielded values in the range 10-30% (e.g., Nestor et al. 2013; Mostardi et al. 2013; Cooke et al. 2014) and several apparent confirmations of bona-fide Lyman-continuum photons (Vanzella et al. 2010; de Barros et al. 2015; Mostardi et al. 2015), follow-up of many of the most promising Lyman-continuum emitter candidates have shown that foreground sources continue to act as a strong source of contamination for such samples (Siana et al. 2015) despite apparently careful efforts to accurately estimate the contamination rate using simulations (Nestor et al. 2013; Mostardi et al. 2013).

Of course, in comparing the escape fraction estimates at $z \sim 2-3$ with the inferred escape fractions at $z > 6$ if galaxies drive the reionization of the universe, we need to keep in mind the fact that there must be some evolution in the escape fraction (e.g., Haardt & Madau et al. 2012; Kuhlen & Faucher-Giguère 2012) to reconcile constraints on the ionizing emissivity at $z = 2-6$ (e.g., Bolton & Haehnelt 2007; Becker & Bolton 2013) with the evolution

observed in the UV luminosity density (e.g., Bouwens et al. 2015a).

4.3. Implications for Escape Fraction Measurements with JWST

In planning for future science endeavors with JWST, there is great interest in devising strategies for measuring the Lyman-continuum escape fraction from $z > 6$ galaxies. One possible approach for measuring the escape fraction was proposed by Zackrisson et al. (2013) and involved using various observed properties of a stellar population, e.g., the observed UV -continuum slopes, to predict the luminosity in various emission lines, particularly $H\beta$, arising from that stellar population. By comparing the predicted luminosity with that expected from accurate stellar population models, one could in principle infer the escape fraction based on an observed deficit in the flux present in key emission lines (i.e., $H\beta$ and sometimes $H\alpha$).

As discussed in §3, there is some uncertainty in the present results for ξ_{ion} – both because of the dependence on the dust law and due to uncertainties on our stack results, i.e., ± 0.02 - 0.09 dex. However, our results bring up an interesting possibility. If current estimates for ξ_{ion} (adopting the SMC extinction law) are correct and the intrinsic value for ξ_{ion} is really in excess of the expected values (based on UV -continuum information available for galaxy samples) and the excess is ~ 0.1 dex, this could be problematic for the aforementioned strategy for measuring the Lyman-continuum escape fraction.

The Zackrisson et al. (2013) strategy, while admittedly clever, relies on our making accurate predictions for the overall output of the Lyman-continuum ionizing photons from the continuum light produced by stars. If the escape fraction is not especially large (and 13% would appear to be an upper limit on its likely value), escaping LyC photons would only impact the $H\beta$ luminosities at the ~ 0.03 dex level. If the intrinsic value for ξ_{ion} cannot be determined at the 0.02 dex level from the observations (much smaller than the tentative ~ 0.1 dex excess we find in ξ_{ion} for SMC dust), then it will be challenging to measure a positive escape fraction at better than 2σ significance.

5. SUMMARY

In this paper, we make use of a large sample of $z \sim 4$ - 5 galaxies for the purposes of estimating the Lyman-continuum photon production efficiency ξ_{ion} . Our selected sources were drawn from the recent $z = 3.8$ - 5.0 Smit et al. (2015b) and $z = 5.1$ - 5.4 Rasappu et al. (2015) selections, who make use of galaxies where the position of the $H\alpha$ line in the IRAC filters with high confidence. The flux in the $H\alpha$ emission line is estimated by comparing the observed flux in the $3.6\mu\text{m}$ or $4.5\mu\text{m}$ bands with the predicted flux in this band based on an SED to the other photometric observations (see Smit et al. 2015b; Rasappu et al. 2015; Shim et al. 2011; Stark et al. 2013 for details). We then use the inferred $H\alpha$ fluxes to estimate the Lyman-continuum photon production efficiency ξ_{ion} for galaxies in this sample.

In deriving the $H\alpha$ flux, we correct for dust extinction based on the observed UV -continuum slopes while alternatively assuming a Calzetti et al. (2000) and SMC extinction laws. The $H\alpha$ emission line is assumed to be

subject to the same dust extinction as the stellar continuum. We also suppose that 6.8% and 9.5% of the flux at the position of the $H\alpha$ emission line is in the [NII] and [SII] lines, based on both theoretical and observational results for the line ratios (Anders & Fritze-v. Alvensleben 2003; Sanders et al. 2015).

By applying this procedure to the $z \sim 4$ - 5 galaxies in the Smit et al. (2015b) and Rasappu et al. (2015) samples, we derive fiducial values of $25.27^{+0.03}_{-0.03}$ and $25.34^{+0.02}_{-0.02}$ for $\log_{10} \xi_{ion}/[\text{Hz ergs}^{-1}]$ assuming the Calzetti and SMC extinction laws, respectively. The value of ξ_{ion} for individual galaxies is estimated to show an intrinsic scatter of ~ 0.3 dex (Figure 4).

This is the first time ξ_{ion} has been estimated from the inferred $H\alpha$ fluxes of $z \geq 4$ galaxies. ~ 0.03 -dex higher values are expected if the escape fraction is non-zero and galaxies provide the dominant contribution to the observed ionizing emissivity at $z \sim 4$ - 5 . The ξ_{ion} values we derive would be higher (0.02-0.09 dex) if we assume that nebular regions are subject to $2.3\times$ higher extinction than the stellar continuum (as has been found in the local universe: Calzetti et al. 1997).

The values we derive for ξ_{ion} in the case of the Calzetti et al. (2000) extinction law are quite consistent with canonical values (Table 2) for all but the bluest sources. For sources with $\beta < -2.3$, we find ξ_{ion} values which are elevated by ~ 0.2 dex relative to canonical values, as predicted by various stellar population models considered in Bouwens et al. (2015b) and Duncan & Conselice (2015).

If the early ALMA results from Capak et al. (2015) are correct and dust extinction follows more of an SMC-like dust law, the Lyman-continuum photon production efficiency ξ_{ion} we infer is also consistent with canonical assumptions in reionization models, but preferring a slightly higher value (by ~ 0.1 dex) than in these models and also as preferred for Calzetti et al. (2000) dust.

The high ξ_{ion} 's we measure for the bluest galaxies in our selection are strikingly similar to those obtained by Stark et al. (2015) on one $z = 7.045$ galaxy, i.e., $\log_{10} \xi_{ion}/[\text{Hz ergs}^{-1}] = 25.68^{+0.27}_{-0.19}$. If these results are representative of $z > 6$ galaxies (and such results were suggested by work by Bouwens et al. 2015b and Duncan & Conselice 2015), this suggests that faint blue galaxies may be especially efficient producers of ionizing radiation.

The present results have important implications, implying that (1) the stellar populations of $z > 2$ galaxies produce Lyman-continuum ionizing photons at the same rate as (or higher than) expected based on standard stellar population models (e.g., Bruzual & Charlot 2003) and (2) indicating that galaxies cannot have an escape fraction substantially higher than 13% unless the UV LF cuts off brightward of -13 mag or the clumping factor is greater than 3 (§4.2). The 13% escape fraction we refer to here is lower than the 20% number often used in conjunction with a Lyman-continuum photon production efficiency of $\log_{10} \xi_{ion}/[\text{Hz ergs}^{-1}] = 25.2$. Unexpectedly high ξ_{ion} 's could be problematic (§4.3) for some proposed strategies for measuring the escape fraction in the reionization epoch using the observed flux in various recombination lines (e.g., Zackrisson et al. 2013).

We expect to extend these results to even lower luminosity galaxies in future work. This is by taking ad-

vantage of a larger sample of $z \sim 3.8$ -5.4 sources with spectroscopic redshifts from MUSE (Bacon et al. 2015) and the very deep 200-hour IRAC observations being acquired over a 200 arcmin² region in the GOODS North and South fields with the GOODS Re-ionization Era wide-Area Treasury from Spitzer (GREATS, PI: Labbé) program (2014). This same regime will also be significantly explored leveraging the lensing amplification achieved behind the Hubble Frontier Fields clusters (e.g., Coe et al. 2015) as well as the deep Spitzer/IRAC observations and MUSE redshift information available there.

This paper is much improved as a result of com-

ments from an expert referee. We are grateful to Jarle Brinchmann for valuable conversations concerning the H α fluxes in galaxies and the robustness of conversions to ionizing photon production rates. This paper benefitted significantly from Brant Robertson's expert comments generously provided pre-submission. We also received valuable feedback regarding current theoretical work in characterizing high-mass stellar evolution (and the dependence on binarity, rotation, etc.) from Selma de Mink and Ylva Götberg. We acknowledge useful discussions with Jorryt Matthee and also support from NASA grant NAG5-7697, NASA grant *HST*-GO-11563, and NWO vrij competitie grant 600.065.140.11N211.

REFERENCES

- Alvarez, M. A., Finlator, K., & Trenti, M. 2012, *ApJ*, 759, LL38
- Anders, P., & Fritze-v. Alvensleben, U. 2003, *A&A*, 401, 1063
- Ashby, M. L. N., Willner, S. P., Fazio, G. G., et al. 2013, *ApJ*, 769, 80
- Ashby, M. L. N., Willner, S. P., Fazio, G. G., et al. 2015, *ApJS*, 218, 33
- Bacon, R., Brinchmann, J., Richard, J., et al. 2015, *A&A*, 575, A75
- Balestra, L., Mainieri, V., Popesso, P., et al. 2010, *A&A*, 512, A12
- Becker, G. D., & Bolton, J. S. 2013, *MNRAS*, 436, 1023
- Bolton, J. S., & Haehnelt, M. G. 2007, *MNRAS*, 382, 325
- Bouchet, P., Lequeux, J., Maurice, E., Prevot, L., & Prevot-Burnichon, M. L. 1985, *A&A*, 149, 330
- Bouwens, R. J., Illingworth, G. D., Blakeslee, J. P., & Franx, M. 2006, *ApJ*, 653, 53
- Bouwens, R. J., Illingworth, G. D., Franx, M., & Ford, H. 2007, *ApJ*, 670, 928
- Bouwens, R. J., Illingworth, G. D., Oesch, P. A., et al. 2011b, *ApJ*, 737, 90
- Bouwens, R. J., Illingworth, G. D., Oesch, P. A., et al. 2012a, *ApJ*, 752, L5
- Bouwens, R. J., Illingworth, G. D., Oesch, P. A., et al. 2012b, *ApJ*, 754, 83
- Bouwens, R. J., Illingworth, G. D., Oesch, P. A., et al. 2014, *ApJ*, 793, 115
- Bouwens, R. J., Illingworth, G. D., Oesch, P. A., et al. 2015a, *ApJ*, 803, 34
- Bouwens, R. J., Illingworth, G. D., Oesch, P. A., et al. 2015b, *ApJ*, 811, 140
- Bouwens, R. J. 2015c, arXiv:1511.01133
- Bradley, L. D., Bouwens, R. J., Zitrin, A., et al. 2012, *ApJ*, 747, 3
- Bruzual, G., & Charlot, S. 2003, *MNRAS*, 344, 1000
- Calzetti, D., Meurer, G. R., Bohlin, R. C., et al. 1997, *AJ*, 114, 1834
- Calzetti, D., Armus, L., Bohlin, R. C., et al. 2000, *ApJ*, 533, 682
- Capak, P. L., Carilli, C., Jones, G., et al. 2015, *Nature*, 522, 455
- Castellano, M., Fontana, A., Grazian, A., et al. 2012, *A&A*, 540, A39
- Charlot, S., & Longhetti, M. 2001, *MNRAS*, 323, 887
- Chen, H.-W., Prochaska, J. X., & Gnedin, N. Y. 2007, *ApJ*, 667, L125
- Coe, D., Bradley, L., & Zitrin, A. 2015, *ApJ*, 800, 84
- Cooke, J., Ryan-Weber, E. V., Garel, T., & Díaz, C. G. 2014, *MNRAS*, 441, 837
- de Barros, S., Schaerer, D., & Stark, D. P. 2014, *A&A*, 563, A81
- de Barros, S., Vanzella, E., Amorín, R., et al. 2015, *ApJ*, in press, arXiv:1507.06648
- de Mink, S. E., Langer, N., Izzard, R. G., Sana, H., & de Koter, A. 2013, *ApJ*, 764, 166
- Dickinson, M., & GOODS Team 2004, *Bulletin of the American Astronomical Society*, 36, #163.01
- Duncan, K., & Conselice, C. J. 2015, *MNRAS*, 451, 2030
- Dunlop, J. S., Rogers, A. B., McLure, R. J., et al. 2013, *MNRAS*, 432, 3520
- Eldridge, J. J., & Stanway, E. R. 2009, *MNRAS*, 400, 1019
- Eldridge, J. J., & Stanway, E. R. 2012, *MNRAS*, 419, 479
- Erb, D. K., Steidel, C. C., Shapley, A. E., et al. 2006, *ApJ*, 647, 128
- Finlator, K., Oh, S. P., Özel, F., & Davé, R. 2012, *MNRAS*, 427, 2464
- Finkelstein, S. L., Papovich, C., Salmon, B., et al. 2012a, *ApJ*, 756, 164
- Finkelstein, S. L., Papovich, C., Ryan, R. E., et al. 2012b, *ApJ*, 758, 93
- Finkelstein, S. L. 2015, *PASA*, in press, arXiv:1511.05558
- Fontana, A., Dunlop, J. S., Paris, D., et al. 2014, *A&A*, 570, A11
- Förster Schreiber, N. M., Genzel, R., Bouché, N., et al. 2009, *ApJ*, 706, 1364
- Gallagher, J. S., III, Hunter, D. A., & Tutukov, A. V. 1984, *ApJ*, 284, 544
- Giallongo, E., Grazian, A., Fiore, F., et al. 2015, *A&A*, 578, A83
- Giavalisco, M., Ferguson, H. C., Koekemoer, A. M., et al. 2004a, *ApJ*, 600, L93
- Gräfenor, G., & Vink, J. S. 2015, *A&A*, 578, L2
- Grogin, N. A., Kocevski, D. D., Faber, S. M., et al. 2011, *ApJS*, 197, 35
- Haardt, F., & Madau, P. 2012, *ApJ*, 746, 125
- Hathi, N. P., Cohen, S. H., Ryan, R. E., Jr., et al. 2013, *ApJ*, 765, 88
- Ishigaki, M., Kawamata, R., Ouchi, M., et al. 2015, *ApJ*, 799, 12
- Kajisawa, M., Konishi, M., Suzuki, R., et al. 2006, *PASJ*, 58, 951
- Kashino, D., Silverman, J. D., Rodighiero, G., et al. 2013, *ApJ*, 777, L8
- Kennicutt, R. C., Jr. 1983, *ApJ*, 272, 54
- Kennicutt, R. C., Jr. 1998, *ARA&A*, 36, 189
- Kewley, L. J., Dopita, M. A., Leitherer, C., et al. 2013, *ApJ*, 774, 100
- Koekemoer, A. M., Faber, S. M., Ferguson, H. C., et al. 2011, *ApJS*, 197, 36
- Kuhlen, M., & Faucher-Giguère, C.-A. 2012, *MNRAS*, 423, 862
- Kurczynski, P., Gawiser, E., Rafelski, M., et al. 2014, *ApJ*, 793, LL5
- Labbé, I., Oesch, P. A., Bouwens, R. J., et al. 2013, *ApJ*, 777, L19
- Labbé, I., Oesch, P. A., Illingworth, G. D., et al. 2014, *Spitzer Proposal*, 11134
- Labbé, I., Oesch, P. A., Illingworth, G. D., et al. 2015, *ApJS*, 221, 23
- Laporte, N., Streblyanska, A., Clement, B., et al. 2014, *A&A*, 562, L8
- Leitherer, C., & Heckman, T. M. 1995, *ApJS*, 96, 9
- Leitherer, C., Ekström, S., Meynet, G., et al. 2014, *ApJS*, 212, 14
- Lequeux, J., Maurice, E., Prevot-Burnichon, M.-L., Prevot, L., & Rocca-Volmerange, B. 1982, *A&A*, 113, L15
- Levesque, E. M., Leitherer, C., Ekstrom, S., Meynet, G., & Schaerer, D. 2012, *ApJ*, 751, 67
- Madau, P., Haardt, F., & Rees, M. J. 1999, *ApJ*, 514, 648
- Madau, P., & Haardt, F. 2015, *ApJ*, 813, L8
- Marmol-Queraltó, E., McLure, R. J., Cullen, F., et al. 2015, *MNRAS*, submitted, arXiv:1511.01911
- Meurer, G. R., Heckman, T. M., & Calzetti, D. 1999, *ApJ*, 521, 64
- Mitra, S., Choudhury, T. R., & Ferrara, A. 2015, *MNRAS*, submitted, arXiv:1505.05507
- Mostardi, R. E., Shapley, A. E., Nestor, D. B., et al. 2013, *ApJ*, 779, 65
- Mostardi, R. E., Shapley, A. E., Steidel, C. C., et al. 2015, *ApJ*, 810, 107

- Nestor, D. B., Shapley, A. E., Kornei, K. A., Steidel, C. C., & Siana, B. 2013, *ApJ*, 765, 47
- Oesch, P. A., Bouwens, R. J., Carollo, C. M., et al. 2010, *ApJ*, 709, L21
- Oesch, P. A., Labbé, I., Bouwens, R. J., et al. 2013, *ApJ*, 772, 136
- Oke, J. B., & Gunn, J. E. 1983, *ApJ*, 266, 713
- Pawlik, A. H., Schaye, J., & van Scherpenzeel, E. 2009, *MNRAS*, 394, 1812
- Pawlik, A. H., Schaye, J., & Dalla Vecchia, C. 2015, *MNRAS*, 451, 1586
- Pentericci, L., Vanzella, E., Fontana, A., et al. 2014, *ApJ*, 793, 113
- Planck Collaboration, Ade, P. A. R., Aghanim, N., et al. 2015, arXiv:1502.01589
- Prevot, M. L., Lequeux, J., Prevot, L., Maurice, E., & Rocca-Volmerange, B. 1984, *A&A*, 132, 389
- Price, S. H., Kriek, M., Brammer, G. B., et al. 2014, *ApJ*, 788, 86
- Ramírez-Agudelo, O. H., Simón-Díaz, S., Sana, H., et al. 2013, *A&A*, 560, A29
- Rasappu, N., Smit, R., Labbé, I., et al. 2015, *MNRAS*, submitted, arXiv:1509.02167
- Reddy, N. A., Erb, D. K., Pettini, M., Steidel, C. C., & Shapley, A. E. 2010, *ApJ*, 712, 1070
- Reddy, N. A., Kriek, M., Shapley, A. E., et al. 2015, *ApJ*, 806, 259
- Robertson, B. E., Furlanetto, S. R., Schneider, E., et al. 2013, *ApJ*, 768, 71
- Robertson, B. E., Ellis, R. S., Furlanetto, S. R., & Dunlop, J. S. 2015, *ApJ*, 802, L19
- Roberts-Borsani, G. W., Bouwens, R. J., Oesch, P. A., et al. 2015, *ApJ*, in press, arXiv:1506.00854
- Rogers, A. B., McLure, R. J., Dunlop, J. S., et al. 2014, *MNRAS*, 440, 3714
- Sana, H., de Mink, S. E., de Koter, A., et al. 2012, *Science*, 337, 444
- Sanders, R. L., Shapley, A. E., Kriek, M., et al., 2015, *ApJ*, 799, 138
- Schaerer, D. 2003, *A&A*, 397, 527
- Schaerer, D., & de Barros, S. 2009, *A&A*, 502, 423
- Schenker, M. A., Ellis, R. S., Konidaris, N. P., & Stark, D. P. 2014, *ApJ*, 795, 20 [S14]
- Shapley, A. E., Steidel, C. C., Pettini, M., Adelberger, K. L., & Erb, D. K. 2006, *ApJ*, 651, 688
- Shivaei, I., Reddy, N. A., Steidel, C. C., & Shapley, A. E. 2015, *ApJ*, 804, 149
- Shim, H., Chary, R.-R., Dickinson, M., et al. 2011, *ApJ*, 738, 69
- Shull, J. M., Harness, A., Trenti, M., & Smith, B. D. 2012, *ApJ*, 747, 100
- Siana, B., Teplitz, H. I., Ferguson, H. C., et al. 2010, *ApJ*, 723, 241
- Siana, B., Shapley, A. E., Kulas, K. R., et al. 2015, *ApJ*, 804, 17
- Skelton, R. E., Whitaker, K. E., Momcheva, I. G., et al. 2014, *ApJS*, 214, 24
- Smit, R., Bouwens, R. J., Labbé, I., et al. 2014, *ApJ*, 784, 58
- Smit, R., Bouwens, R. J., Franx, M., et al. 2015a, *ApJ*, 801, 122
- Smit, R., Bouwens, R. J., Labbé, I., et al. 2015b, *ApJ*, submitted, arXiv:1511.08808
- Stanway, E. R., Eldridge, J. J., & Becker, G. D. 2015, arXiv:1511.03268
- Stark, D. P., Ellis, R. S., Chiu, K., Ouchi, M., & Bunker, A. 2010, *MNRAS*, 408, 1628
- Stark, D. P., Ellis, R. S., & Ouchi, M. 2011, *ApJ*, 728, L2
- Stark, D. P., Schenker, M. A., Ellis, R., et al. 2013, *ApJ*, 763, 129
- Stark, D. P., Walth, G., Charlot, S., et al. 2015, *MNRAS*, 454, 1393
- Steidel, C. C., Pettini, M., & Adelberger, K. L. 2001, *ApJ*, 546, 665
- Szécsi, D., Langer, N., Yoon, S.-C., et al. 2015, *A&A*, 581, A15
- Topping, M. W., & Shull, J. M. 2015, *ApJ*, 800, 97
- Vanzella, E., Cristiani, S., Dickinson, M., et al. 2005, *A&A*, 434, 53
- Vanzella, E., Cristiani, S., Dickinson, M., et al. 2006, *A&A*, 454, 423
- Vanzella, E., Cristiani, S., Dickinson, M., et al. 2008, *A&A*, 478, 83
- Vanzella, E., Giavalisco, M., Dickinson, M., et al. 2009, *ApJ*, 695, 1163
- Vanzella, E., Siana, B., Cristiani, S., & Nonino, M. 2010a, *MNRAS*, 404, 1672
- Vanzella, E., Giavalisco, M., Inoue, A. K., et al. 2010b, *ApJ*, 725, 1011
- Wilkins, S. M., Bouwens, R. J., Oesch, P. A., et al. 2015, *MNRAS*, in press, arXiv:1510.01514
- Windhorst, R. A., Cohen, S. H., Hathi, N. P., et al. 2011, *ApJS*, 193, 27
- Yan, H., & Windhorst, R. A. 2004, *ApJ*, 612, L93
- Yoon, S.-C., Langer, N., & Norman, C. 2006, *A&A*, 460, 199
- Zackrisson, E., Inoue, A. K., & Jensen, H. 2013, *ApJ*, 777, 39